2023 62nd IEEE Conference on Decision and Control (CDC)
December 13-15, 2023. Marina Bay Sands, Singapore

Fully Distributed Dynamic Event-triggering Formation Control of UAV Swarms under DoS Attacks

Hui Cao[1,2], Liang Han[2], Dongyu Li[1,3*], Qinglei Hu[1,4], and Pengkun Hao[2]

***Abstract*— For large-scale unmanned aerial vehicle (UAV) swarms, the security of communication networks is critical. When subjected to cyberattacks, the performance of swarm systems will be significantly affected. This paper focuses on the fully distributed time-varying formation (TVF) control problem of UAV swarms under Denial-of-Service (DoS) attacks. First, the theoretical framework of the fully distributed dynamic event-triggering TVF control protocol is introduced. Then, sufficient conditions and critical proofs are provided to demonstrate that the desired formation configuration can be achieved under the influence of DoS attacks, and Zeno behavior is eliminated. Finally, the framework of a mixed-reality swarm flight platform is presented, which includes virtual nodes and physical nodes and integrates the advantages of both simulation and physical experiments, enabling large-scale swarm experiments with less cost and higher efficiency. The formation experiment using this platform validates the efficacy of the proposed control protocol.**

I. INTRODUCTION

With the rapid advancement of autonomous robots, unmanned aerial vehicles (UAVs) have shown application prospects in many fields, such as delivery logistics [1], smart farming [2], firefighting [3], and environmental exploration [4]. Compared with a single UAV, UAV swarms have distributed sensing, computing, and execution capabilities, which can complete tasks that cannot be accomplished by a single UAV. As an important part of the cooperative control problem, the formation control problem has been widely studied, such as leaderless formation [5]–[7], leader-follower formation [8]–[10], and formation containment [11]–[13]. Good cooperative control effects rely on stable and reliable communication between UAVs, especially in large-scale UAV swarms. However, the UAV wireless network is prone to various malicious threats, such as Denial-of-Service (DoS) attacks [14]–[16].

This work was supported by Tianmushan Laboratory Research Project TK-2023-C-020 and TK-2023-B-010, the National Natural Science Foundation of China under Grants 62103028 and 61803014, the Zhejiang Provincial Natural Science Foundation of China under Grants LGG22F030025 and LGG22F030018, the Key Laboratory of Industrial Internet of Things & Networked Control, Ministry of Education under Project 2022FF04, and the Fundamental Research Funds for the Central Universities.

[1]H. Cao, D. Li, and Q. Hu are with Tianmushan Laboratory, Hangzhou, 310023, China. caohui@buaa.edu.cn; dongyuli@buaa.edu.cn;huql_buaa@buaa.edu.cn

[2]H. Cao, L. Han, and P. Hao are with the Sino-French Engineer School, Beihang University, Beijing, 100191, China. liang_han@buaa.edu.cn;haopengkun1724@163.com

[3]D. Li is also with the School of Cyber Science and Technology, Beihang University, Beijing, 100191, China.

[4]Q. Hu is also with the School of Automation Science and Electrical Engineering, Beihang University, Beijing, 100191, China.

*Corresponding author.

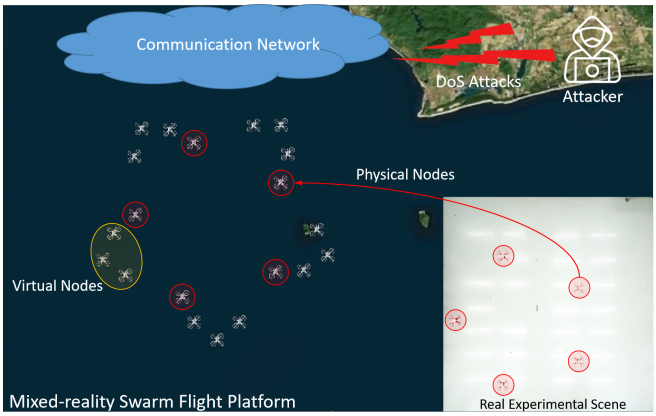

Fig. 1: Illustration of the mixed-reality swarm experiment under DoS attacks (quadrotors in red circles are physical ones, while those in yellow circles are virtual ones).

This paper focuses on the time-varying formation (TVF) control problem of UAV swarms under DoS attacks, which may block or destroy the communication channels between UAVs, thus causing packet dropout or even the swarm system to lose control. Some researches have been done on the cooperative control of swarm systems under DoS attacks. In [17], a distributed output-feedback control approach is proposed to solve the output consensus problem of heterogeneous multi-agent systems (MASs) with random DoS attacks. The paper [18] designs a state-feedback controller based on switched time-delay system method for the connected vehicles to follow a desired speed while maintaining a desired vehicle spacing under aperiodic DoS attacks. The paper [19] solves the leader-follower consensus problem of MASs suffering from time-varying delay and DoS attacks.

UAV swarms are generally composed of multiple tiny embedded systems. Thus, the computing capacity, communication bandwidth, and battery capacity of each UAV are limited. In the theoretical research of formation control, communication in a swarm system is usually assumed to be continuous, where sufficient computing resources and an ideal communication environment are required. Besides, the periodic sampling communication mechanism is often adopted. Although this mechanism is easier to implement, it will waste communication resources, especially when the closed-loop system tends to be stable. Moreover, a small sampling period may cause a large number of redundant system sampling states to be released into the communication network, which may lead to network congestion or even the collapse of embedded systems [20]. To solve

these problems, event-triggering communication mechanisms are introduced into cooperative control of swarm systems [21]–[23]. Compared with a fixed sampling period, event-triggering mechanisms rely on a predefined event-triggering condition (ETC). Only when the ETC is satisfied can the UAV communicate with its neighbors, and the exchange of information happens, which may effectively save the communication and computing resources and prolong the life of UAVs.

Moreover, it is worth noting that most of the current research on the cooperative control problem of swarm systems under DoS attacks is not fully distributed. Some global information, such as the Laplace matrix of the communication topology among UAVs or its eigenvalues, is required in the control protocol design (e.g., [17]–[19]). However, global information may be difficult to obtain in practical applications, and changes may happen during the process. In addition, the computing resources onboard are limited, while the processing of some global information needs a lot of computing resources, for example, the computation of eigenvalues of the Laplace matrix for a large network. Therefore, a fully distributed control protocol is needed because of its stronger robustness, better flexibility, and higher reliability.

Inspired by the above discussions, this paper focuses on the fully distributed TVF control protocol design of UAV swarms based on the dynamic event-triggering mechanism under DoS attacks. The main contributions are listed as follows:

1) A fully distributed dynamic event-triggering TVF control framework considering DoS attacks is established. Experimental results with five physical quadrotors and fifteen virtual quadrotors are presented to validate the effectiveness of the proposed control protocol.
2) The duration and frequency of DoS attacks that can be tolerated are analyzed. Critical proofs are given to demonstrate the resilience of the protocol proposed under DoS attacks.
3) A mixed-reality swarm flight platform is proposed, which includes physical nodes and virtual nodes, breaking through the limitations of experimental sites, hardware facilities, etc., and enabling swarm algorithms to be verified on large-scale swarms.

II. PROBLEM DESCRIPTION

In this section, some preliminaries related to algebraic graph theory are introduced and mathematical models for DoS attacks, dynamics of UAVs, and formations are established, which lays the foundation of the subsequent analysis of this paper.

A. Preliminaries

Consider a swarm system of N UAVs, whose communication relationship is represented by an undirected graph $\mathscr{G} = \{\mathscr{V}, \mathscr{E}\}$ with $\mathscr{V} = \{1, 2, \cdots, N\}$ the node set and $\mathscr{E} \subseteq \mathscr{V} \times \mathscr{V}$ the edge set. Denote $\mathscr{A} = [a_{ij}] \in \mathbb{R}^{N\times N}$ the adjacency matrix of $\mathscr{G}$, in which $a_{ij} = 1$ if and only if $(i, j) \in \mathscr{E}$; otherwise, $a_{ij} = 0$. The set of neighbors of UAV i is represented by $\mathscr{N}_i = \{j \in \mathscr{V} \mid (i, j) \in \mathscr{E}\}$. Assume that there exists no self loop in $\mathscr{G}$, i.e., $a_{ii} = 0$. The Laplacian matrix of $\mathscr{G}$ is denoted by $\mathscr{L} = [l_{ij}] \in \mathbb{R}^{N\times N}$ with $l_{ij} = -a_{ij}$, $i \neq j$ and $l_{ii} = \sum_{j=1}^{N} a_{ij}$.

Assumption 1: The communication graph $\mathscr{G}$ of the UAV swarm is undirected and connected.

Lemma 1 ([24]): The Laplacian matrix $\mathscr{L}$ of an undirected and connected graph $\mathscr{G}$ has a simple eigenvalue 0 and $N-1$ positive eigenvalues, i.e., $\lambda_1 = 0$ and $0 < \lambda_2 \leq \cdots \leq \lambda_N$.

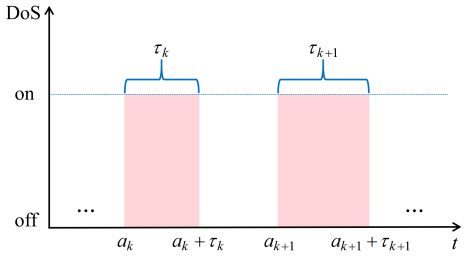

Fig. 2: An illustration of DoS attacks launched on the communication network.

B. DoS attacks

Define the sequences $\{a_k \geq 0\}_{k\in\mathbb{N}}$ and $\{\tau_k \geq 0\}_{k\in\mathbb{N}}$ to represent the start time instants and the durations of DoS attacks, respectively. As shown in Fig.2, a_k represents the start time instant for the kth attack, and τ_k represents its duration. For each $k \in \mathbb{N}$, it is assumed that $a_{k+1} > a_k + \tau_k$.

Denote by $\mathscr{A}_k \triangleq [a_k, a_k + \tau_k]$ the kth attack interval, during which all transmissions of the communication channels between the UAVs are prevented. For any time interval $[t_1, t_2] \subset [0, \infty)$, $\overline{\mathscr{A}}(t_1, t_2)$ is used to represent the set of times under DoS attacks, that is, $\overline{\mathscr{A}}(t_1, t_2) \triangleq \cup_{k\in\mathbb{N}} \mathscr{A}_k \cap [t_1, t_2]$. Moreover, we use $\overline{\mathscr{A}}^c(t_1, t_2)$ to denote the complement of $\overline{\mathscr{A}}(t_1, t_2)$, that is, $\overline{\mathscr{A}}^c(t_1, t_2) \triangleq [t_1, t_2] \backslash \overline{\mathscr{A}}(t_1, t_2)$, in which there is no attack.

Assumption 2 (Attack Duration): For any $t_2 > t_1 \geq 0$, there exists $T_0 \geq 0$ and $1/\tau_a \in (0, 1)$ such that the total DoS attack duration $|\overline{\mathscr{A}}(t_1, t_2)|$ satisfies:

$$|\overline{\mathscr{A}}(t_1, t_2)| \leq T_0 + \frac{t_2 - t_1}{\tau_a}, \tag{1}$$

where $|\overline{\mathscr{A}}(t_1, t_2)|$ represents the total duration of the attacks in the interval $[t_1, t_2]$.

Assumption 3 (Attack Frequency): For any $t_2 > t_1 \geq 0$, denote the total number of DoS attacks in the time interval $[t_1, t_2]$ as $N_f(t_1, t_2)$, and there exists $F_f > 0$ such that

$$N_f(t_1, t_2) \leq F_f \cdot (t_2 - t_1). \tag{2}$$

C. Problem statement

On the formation control level, the dynamics of the UAV i can be described as the following double-integrator [12]

$$\begin{cases} \dot{p}_i(t) = v_i(t), \\ \dot{v}_i(t) = u_i(t), \end{cases} \tag{3}$$

where $i \in \{1, 2, \cdots, N\}$, $p_i(t) \in \mathbb{R}^n$, $v_i(t) \in \mathbb{R}^n$, and $u_i(t) \in \mathbb{R}^n$ denot the position vector, the velocity vector, and the control input of UAV i at time instant t, respectively. For simplicity, n is assumed to be 1 in the following description, if not

otherwise specified. However, it should be noted that the results are still available for the cases $n > 1$ by using the Kronecker product. Define $x_i(t) = [p_i(t), v_i(t)]^T$. Then, the dynamics (3) can be rewritten as

$$\dot{x}_i(t) = Ax_i(t) + Bu_i(t), \tag{4}$$

where $A = \begin{bmatrix} 0 & 1 \\ 0 & 0 \end{bmatrix}$ and $B = \begin{bmatrix} 0 & 1 \end{bmatrix}^T$.

The desired TVF configuration for UAV swarms is denoted by $\phi(t) = [\phi_1^T(t), \phi_2^T(t), \cdots, \phi_N^T(t)]^T$, with $\phi_i(t) \in \mathbb{R}^2$ the piecewise continuously differentiable formation vector for UAV i. Define the following formation feasibility condition:

$$A\phi_i(t) - \dot{\phi}_i(t) + B\tau_i(t) = 0, \tag{5}$$

where $\tau_i(t)$ is the formation compensation input for UAV i. If there exists $\tau_i(t)$ satisfying (5) for all the formation vectors $\phi_i(t)$, then the formation configuration $\phi(t)$ is said to be feasible, otherwise, the expected formation is not feasible.

Definition 1: The UAV swarm (3) is said to achieve desired formation configurations if for any intial value $x_i(t_0) \in \mathbb{R}^2$, the formation error $e(t) \triangleq [e_1^T(t), e_2^T(t), \cdots, e_N^T(t)]^T$, with $e_i(t) = \theta_i(t) - \frac{1}{N}\sum_{j=1}^N \theta_j(t)$, converges to a set S:

$$S = \{e(t) : \|e(t)\| \le s\}, \tag{6}$$

where $\theta_i(t) = x_i(t) - \phi_i(t)$ and s is a constant.

Remark 1: The Laplace matrix property in Lemma 1 is only utilized in the proof. The control protocol design does not rely on the global information of the communication topology and is fully distributed. The proposed limits in Assumptions 2 and 3 align with real situations. If repeated and prolonged DoS attacks occur, neighboring UAVs' data may become unavailable, hindering collaboration and formation. Additionally, such attacks require continuous energy supply from malicious adversaries, which is unrealistic.

III. Main Results

In this section, a complete theoretical framework of the fully distributed dynamic event-triggering TVF control protocol for UAV swarms is established (as shown in Fig.3). Sufficient conditions are given to demonstrate that the control protocol is resilient to DoS attacks. Zeno behavior is also excluded, that is to say, there does not exist infinite triggers in any finite period of time [23].

A. Dynamic Event-triggering Mechanism

The dynamic event-triggering mechanism established in this paper is asynchronous and edge-based. Each UAV can determine its communication instants with each of its neighbors separately, and the communication instants between two neighbors linked by an edge can also be different. Denote by $0 \le t_0^{i\to j} < t_1^{i\to j} < \cdots < t_s^{i\to j} < \cdots$ the asynchronous triggering time sequence, in which UAV i transmits its information to UAV j. During the time interval $[t_k^{i\to j}, t_{k+1}^{i\to j})$, UAV j estimates the state information of UAV i by the following observer:

$$\begin{cases} \dot{\tilde{\theta}}_i^j(t) = A\tilde{\theta}_i^j(t), & t \in [t_k^{i\to j}, t_{k+1}^{i\to j}), \\ \tilde{\theta}_i^j(t) = \theta_i(t_k^{i\to j}), & t = t_k^{i\to j}. \end{cases} \tag{7}$$

Thus, $\tilde{\theta}_i^j(t) = e^{A(t-t_k^{i\to j})}\theta_i(t_k^{i\to j})$, for $t \in [t_k^{i\to j}, t_{k+1}^{i\to j})$. Define the observer error from UAV i to UAV j by

$$e_i^j(t) = \tilde{\theta}_i^j(t) - \theta_i(t),\ t \in [t_k^{i\to j}, t_{k+1}^{i\to j}). \tag{8}$$

An event-triggering function $\mathscr{H}_i^j(\cdot,\cdot,\cdot) : \mathbb{R}^2 \times \mathbb{R}^2 \times \mathbb{R}^2 \to \mathbb{R}$ is designed as follows

$$\begin{aligned} &\mathscr{H}_i^j(e_i^j(t), c_{ij}(t), \tilde{\eta}_{ij}(t)) \\ &= \gamma_{ij}a_{ij}[(1+\varepsilon_{ij}c_{ij}(t))e_i^{jT}(t)\Gamma e_i^j(t) - \iota_{ij}\tilde{\eta}_{ij}^T(t)\Gamma\tilde{\eta}_{ij}(t)], \end{aligned} \tag{9}$$

where $\tilde{\eta}_{ij}(t) = \tilde{\theta}_i^j(t) - \tilde{\theta}_j^i(t)$, $\varepsilon_{ij} \ge 1$, $\iota_{ij} \in (0, \frac{1}{4})$, $\gamma_{ij} > 0$, and the gain matrix $\Gamma \in \mathbb{N}^{2\times 2}$ is to be designed later. The adaptive coupling weight $c_{ij}(t)$ is updated as follows

$$\dot{c}_{ij}(t) = \pi_{ij}a_{ij}[\tilde{\eta}_{ij}^T(t)\Gamma\tilde{\eta}_{ij}(t) - \beta_{ij}c_{ij}(t)], \tag{10}$$

where $\pi_{ij} = \pi_{ji} > 0$, $\beta_{ij} = \beta_{ji} > 0$, $c_{ij}(0) = c_{ji}(0) > 0$ for $(i,j) \in \mathscr{E}$, and $c_{ij}(0) = c_{ji}(0) = 0$ for $(i,j) \notin \mathscr{E}$. It is obvious that $c_{ij}(t) = c_{ji}(t)$ with $t \ge 0$. The next event-triggering time instant $t_{k+1}^{i\to j}$ of UAV i to UAV j is updated by the following dynamic event-triggering condition:

$$\begin{aligned} t_{k+1}^{i\to j} = \inf_{l > t_k^{i\to j}} \{l : \mathscr{H}_i^j(e_i^j(t), c_{ij}(t), \tilde{\eta}_{ij}(t)) > a_{ij}\delta_{ij}(t), \\ \forall t \in (t_k^{i\to j}, l]\}, \end{aligned} \tag{11}$$

for $\forall i \in \mathscr{V}$, $j \in \mathscr{N}_i$, where $\delta_{ij}(t)$ is the dynamic threshold determined by

$$\dot{\delta}_{ij}(t) = -a_{ij}\alpha_{ij}\delta_{ij}(t) - \frac{\mu_{ij}}{\gamma_{ij}}\mathscr{H}_i^j(e_i^j(t), c_{ij}(t), \tilde{\eta}_{ij}(t)), \tag{12}$$

with $\alpha_{ij} > \frac{1-\mu_{ij}}{\gamma_{ij}}$, $\mu_{ij} \in (0,1)$, and $\delta_{ij}(0)$>0.

B. Fully distributed TVF Controller

Under the dynamic event-triggering mechanism presented in (9)-(12), a fully distributed TVF controller is designed as follows

$$u_i(t) = K\sum_{j=1}^N a_{ij}c_{ij}(t)\tilde{\eta}_{ji}(t) + \tau_i(t), \tag{13}$$

where $K \in \mathbb{R}^{1\times 2}$ is the feedback gain matrix to be determined later, and $\tau_i(t)$ is the formation compensation input defined in (5). According to (4), (5), and (13), we have

$$\dot{e}_i(t) = Ae_i(t) + B\bar{u}_i(t), \tag{14}$$

with $\bar{u}_i(t) = K\sum_{j=1}^N a_{ij}c_{ij}\tilde{\eta}_{ji}(t)$, for $i \in \mathscr{V}$. To determine gain matrices, a positive definite matrix P is introduced by solving the following algebraic Riccati equation:

$$A^TP + PA - PBB^TP + \sigma_1 I_n = 0, \tag{15}$$

with $\sigma_1 > 0$. Thus, Γ and K are designed as $\Gamma = PBB^TP$ and $K = B^TP$, respectively.

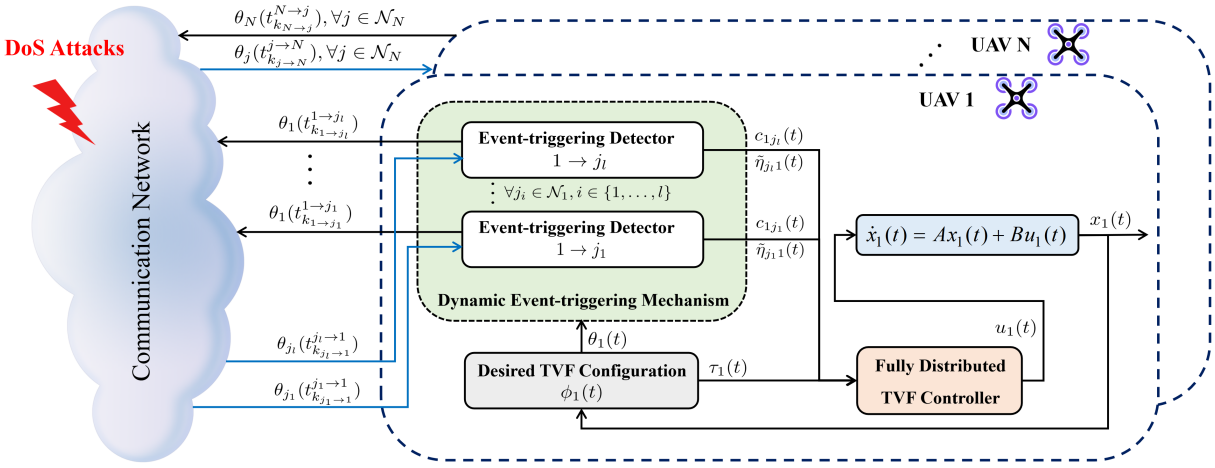

Fig. 3: Theoretical framework of the fully distributed dynamic event-triggering TVF control protocol.

C. Stability Analysis

Theorem 1: Suppose that Assumptions 1-3 hold, and the desired formation configuration satisfies the formation feasibility condition (5). There exists $\kappa^* \in (0, \kappa_1)$ such that the duration and frequency of the attack satisfy

$$\frac{1}{\tau_a} < \frac{\kappa_1 - \kappa^*}{\kappa_1 + \kappa_2}, \tag{16}$$

and

$$\frac{N_f(t_0,t)}{t-t_0} \le \frac{\kappa^*}{(\kappa_1+\kappa_2)\Delta} = F_f, \tag{17}$$

where $\kappa_1 = \min_{(i,j)\in\mathcal{E}}\left\{\beta_{ij}\pi_{ij}, \frac{\alpha_{ij}}{2} - \frac{1-\mu_{ij}}{2\gamma_{ij}}, \frac{\sigma_1}{\lambda_{\max}(P)}\right\} > 0$, $\kappa_2 = \sigma_2 > 0$ satisfying $A^TP + PA - \sigma_2 P \le 0$, and Δ is the time required to recover communication. Then, under the fully distributed dynamic event-triggering TVF control protocol (9)-(13), the UAV swarm (3) suffering from DoS attacks reaches the desired TVF configuration. Futhermore, Zeno behavior is excluded.

Proof: The proof is relatively long and is included in the appendix for clarity. ■

IV. MIXED-REALITY SWARM EXPERIMENT

In this section, a mixed-reality swarm flight platform is presented, and an experiment with five physical quadrotors and fifteen virtual quadrotors is demonstrated.

A. Platform Description

Limited by practical factors such as experimental sites, equipment, and funds, it is difficult to carry out large-scale swarm physical experiments. To overcome these problems, we design a mixed-reality swarm flight platform (as shown in Fig.4). The platform mainly includes four parts: swarm algorithm, virtual nodes, physical nodes, and 3D visual display engine. The swarm algorithm is implemented in the ground control station (GCS). First, the swarm algorithm receives the state information of physical quadrotors from OptiTrack's motion capture system, which is composed of 12 high-precision cameras, and that of virtual quadrotors calculated by double-integrators. Next, the swarm algorithm treats the states of physical quadrotors and virtual quadrotors in the same way and calculates the control commands for each quadrotor through the fully distributed dynamic event-triggering control protocol proposed above. Then, the commands are sent to the physical and virtual nodes. After receiving the commands, the physical quadrotors fly according to the commands and the virtual nodes calculate their next states. Finally, the state information of physical quadrotors and the virtual quadrotors are sent to the 3D visual display engine during the entire flight process.

B. Experimental Results

Consider a swarm system containing twenty quadrotors, five of which are physical ones and fifteen are virtual ones. The movements of quadrotors are set in the X-Y plane. The communication relationship among quadrotors are presented in Fig.5. Choose $\sigma_1 = 16$ and $\sigma_2 = 2.5$. By solving (15), we get the gain matrices $\Gamma = \mathrm{I}_2 \otimes \begin{bmatrix} 196.00 & 209.53 \\ 209.53 & 224.00 \end{bmatrix}$ and $K = \mathrm{I}_2 \otimes \begin{bmatrix} 14.00 & 14.97 \end{bmatrix}$.

The desired TVF configuration $\phi_i(t)$ for UAV i is described as

$$\begin{bmatrix} r\cos(\omega t + d_{1i}) \\ b^2 d\omega \sin(2d\omega t + d_{2i})\cos(\omega t + d_{1i}) - \omega r \sin(\omega t + d_{1i}) \\ r\sin(\omega t + d_{1i}) \\ b^2 d\omega \sin(2d\omega t + d_{2i})\sin(\omega t + d_{1i}) + \omega r \cos(\omega t + d_{1i}) \end{bmatrix},$$

where $i \in \{1,2,\cdots,20\}$, $r = a - 0.5b^2 - 0.5\cos(2d\omega t + d_{2i})$, $d_{1i} = 0.2\pi - 0.1\pi[(i-1) \bmod 4] + 0.4\pi\lfloor\frac{i-1}{4}\rfloor$, $d_{2i} = \pi - 0.5\pi[(i-1) \bmod 4]$, $a = 1$, $b = 0.6$, $\omega = 0.15$, and $d = 2.5$.

The triggering sequence $\{t_k^{i\to j}\}_{k\in\mathbb{N}}$ is determined by the asynchronous dynamic event-triggering mechanism (9)-(12) with $\gamma_{ij} = 1$, $\varepsilon_{ij} = 1$, $\iota_{ij} = 0.24$, $\alpha_{ij} = 1.5$, $\mu_{ij} = 0.6$, $\pi_{ij} = 0.2$, and $\beta_{ij} = 2$. DoS attacks are random and satisfy the conditions in Assumptions 2-3, where the limitations of τ_a and N_f are given in Theorem 1 with $\Delta = 0.01$. The step size of the program is set to be 0.01s.

In Fig.6 and Fig.7, the pink area denotes the time intervals under DoS attacks. Fig.6 shows the change curves of dynamic thresholds, adaptive coupling weights, and the

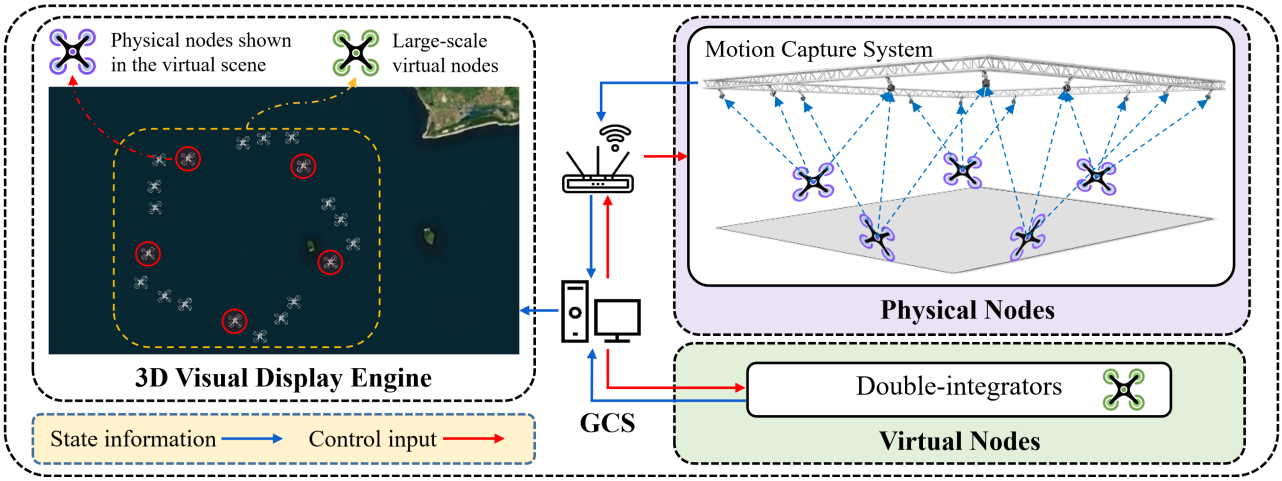

Fig. 4: Overall architecture of the mixed-reality swarm flight platform.

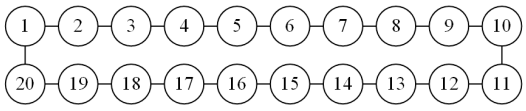

Fig. 5: Communication topology.

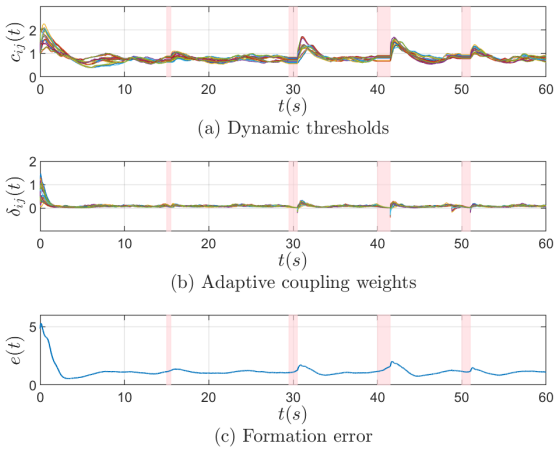

Fig. 6: The curves for parameter change within 60s in mixed-reality experiment.

formation error within 60s, where the formation error is denoted by $e(t) = \sum_{i=1}^{20} \|e_i(t)\|$ with $e_i(t) = \theta_i(t) - \frac{1}{20}\sum_{j=1}^{20} \theta_j(t)$ and $\theta_i(t) = x_i(t) - \phi_i(t)$. Fig.7 presents the triggering time instants of information transmission among quadrotors, from which we can see that the number of communications is greatly reduced. Fig.8 shows the position snapshots from an overhead view of both the 3D virtual display engine and the real experimental scene at $t = 0$s, $t = 15$s, $t = 30$s, and $t = 60$s, where the quadrotors in red circles represent the physical ones. At $t = 0s$, the initial positions of virtual quadrotors are set to zero. It is noticed that the desired TVF configuration is achieved. The video of the experiment is available at https://youtu.be/gYDhr4eLeiY.

C. Analysis and Summary

In this section, the effectiveness of the proposed fully distributed dynamic event-triggering TVF control protocol

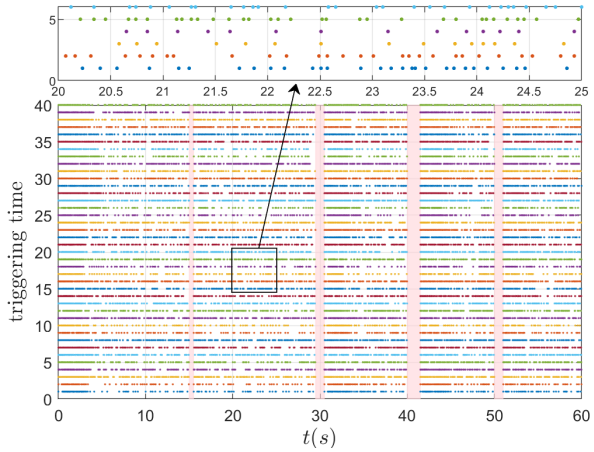

Fig. 7: Triggering time instants within 60s in mixed-reality experiment.

for UAV swarms under DoS attacks is validated by an experiment on twenty quadrotors using the mixed reality swarm flight platform. Compared with pure physical experiments, this mixed-reality swarm flight platform takes advantage of simulation, which facilitates algorithm verification on large-scale UAV swarms with less experimental cost and higher efficiency. Moreover, some physical nodes are introduced such that the effectiveness of swarm algorithms on physical UAVs can be verified compared to pure simulation. In this platform, the dynamics of the virtual UAVs are now double-integrators. In the next step, the parameters of the UAV dynamics will be obtained through system identification, which is more meaningful for the verification of algorithms.

V. CONCLUSION

This paper focuses on the fully distributed TVF control problem of UAV swarms under DoS attacks. To reduce the consumption of communication resources, an asynchronous dynamic event-triggering mechanism is integrated into the design of the fully distributed TVF control protocol, which increases its potential to be applied to large-scale swarm systems. In the end, a mixed-reality swarm flight platform is

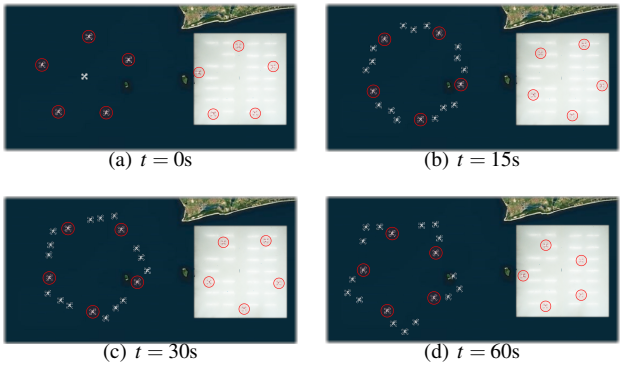

(a) $t = 0$s (b) $t = 15$s (c) $t = 30$s (d) $t = 60$s

Fig. 8: Position snapshots of the 3D virtual display engine and the real experimental scene (quadrotors in red circles are the physical ones).

presented, and an experiment using five physical quadrotors and fifteen virtual quadrotors is conducted to validate the efficacy of the proposed protocol.

APPENDIX

This part provides the proof of Theorem 1.

Firstly, we prove that the desired TVF configuration can be achieved under DoS attacks with the proposed control protocol (9)-(13). To be more concise, the time variable (t) is omitted in this part.

The following discussion considers the case $t \in \overline{\mathscr{A}}^c(t_1,t_2)$, in which the communication channels among agents are not subject to DoS attacks.

Define the following Lyapunov function

$$V(e,\rho) = \frac{1}{2}\sum_{i=1}^{N} e_i^T P e_i + \sum_{i=1}^{N}\sum_{j=1}^{N} \frac{(c_{ij}-\alpha_0)^2}{8\pi_{ij}}, \tag{18}$$

where $\rho = [\rho_1^T,\cdots,\rho_N^T]^T$ with $\rho_i = [c_{i1},\cdots,c_{iN}]^T$, $i \in \mathscr{V}$. α_0 is a constant satisfying $\alpha_0 \geq \min\left\{1, \frac{2q_0}{(1-4\iota)\lambda_2}\right\} > 0$, where $\iota = \max_{(i,j)\in\mathscr{E}}\{\iota_{ij}\}$, λ_2 is the smallest nonzero eigenvalue of $\mathscr{L}$, and $q_0 > 0$ is a constant to be designed later. By using (10) and (14), the time derivative of $V(e,\rho)$ can be obtained as follows

$$\begin{aligned}\dot{V}(e,\rho) = {}& \frac{1}{2}\sum_{i=1}^{N} e_i^T(PA+A^TP)e_i + \sum_{i=1}^{N}\sum_{j=1}^{N} a_{ij}c_{ij}e_i^T\Gamma\tilde{\eta}_{ji} \\ & + \sum_{i=1}^{N}\sum_{j=1}^{N} a_{ij}\frac{c_{ij}-\alpha_0}{4}\tilde{\eta}_{ij}^T\Gamma\tilde{\eta}_{ij} - \sum_{i=1}^{N}\sum_{j=1}^{N} a_{ij}\frac{c_{ij}-\alpha_0}{4}\beta_{ij}c_{ij}. \end{aligned}\tag{19}$$

Since $a_{ij} = a_{ji}$, $c_{ij} = c_{ji}$, $\tilde{\eta}_{ij} = -\tilde{\eta}_{ji}$ with $t \geq 0$, and $e_i - e_j = \theta_i - \theta_j = [\tilde{\theta}_i^j - e_i^j] - [\tilde{\theta}_j^i - e_j^i] = \tilde{\eta}_{ij} - [e_i^j - e_j^i]$, we can obtain that

$$\begin{aligned}\sum_{i=1}^{N}\sum_{j=1}^{N} a_{ij}c_{ij}e_i^T\Gamma\tilde{\eta}_{ji} &= \frac{1}{2}\sum_{i=1}^{N}\sum_{j=1}^{N} a_{ij}c_{ij}[e_i-e_j]^T\Gamma\tilde{\eta}_{ji} \\ &= -\sum_{i=1}^{N}\sum_{j=1}^{N} a_{ij}c_{ij}\left(\frac{1}{2}\tilde{\eta}_{ij}^T\Gamma\tilde{\eta}_{ij} - e_i^{jT}\Gamma\tilde{\eta}_{ij}\right) \\ &\leq \sum_{i=1}^{N}\sum_{j=1}^{N} a_{ij}c_{ij}\left(e_i^{jT}\Gamma e_i^j - \frac{1}{4}\tilde{\eta}_{ij}^T\Gamma\tilde{\eta}_{ij}\right). \end{aligned}\tag{20}$$

Substituting (20) into (19), we obtain that

$$\begin{aligned}\dot{V}(e,\rho) \leq {}& \frac{1}{2}\sum_{i=1}^{N} e_i^T(PA+A^TP)e_i - \sum_{i=1}^{N}\sum_{j=1}^{N} a_{ij}\frac{\alpha_0}{4}\tilde{\eta}_{ij}^T\Gamma\tilde{\eta}_{ij} \\ & + \sum_{i=1}^{N}\sum_{j=1}^{N} a_{ij}c_{ij}e_i^{jT}\Gamma e_i^j - \sum_{i=1}^{N}\sum_{j=1}^{N} a_{ij}\beta_{ij}\frac{(c_{ij}-\alpha_0)^2}{8} + \varsigma, \end{aligned}\tag{21}$$

where $\varsigma = \sum_{i=1}^{N}\sum_{j=1}^{N} a_{ij}\beta_{ij}\frac{\alpha_0^2}{8}$.

From (11) and (12), we have $\dot{\delta}_{ij} \geq -(\alpha_{ij} + \frac{\mu_{ij}}{\gamma_{ij}})\delta_{ij}$, $\forall t \geq 0$. Obviously, $\delta_{ij} \geq \delta_{ij}(0)\exp\{-(\alpha_{ij}+\frac{\mu_{ij}}{\gamma_{ij}})t\} > 0$, $\forall t \geq 0$. Define the following Lyapunov function

$$W(e,\rho,\delta) = V(e,\rho) + \sum_{i=1}^{N}\sum_{j=1}^{N}\alpha_0\delta_{ij}, \tag{22}$$

where $\delta = [\delta_1^T,\cdots,\delta_N^T]^T$ with $\delta_i = [\delta_{i1},\cdots,\delta_{iN}]^T$, $i \in \mathscr{V}$. Notice that $W > 0$ if and only if $(e_i, c_{ij}-\alpha_0, \delta_{ij}) \neq (0,0,0)$ due to $P > 0$ and $\delta_{ij} > 0$. Since $\alpha_0 \geq 1$ and $\varepsilon_{ij} \geq 1$, it is easy to get that

$$\begin{aligned}&\sum_{i=1}^{N}\sum_{j=1}^{N}(c_{ij}-\alpha_0\mu_{ij}(1+\varepsilon_{ij}c_{ij}))a_{ij}e_i^{jT}\Gamma e_i^j \\ &\leq \sum_{i=1}^{N}\sum_{j=1}^{N}\alpha_0(1-\mu_{ij})(1+\varepsilon_{ij}c_{ij})a_{ij}e_i^{jT}\Gamma e_i^j. \end{aligned}\tag{23}$$

In the light of (12), (21), (23), and the dynamic event-triggering condition (11), the time derivative of $W(e,\rho,\delta)$ can be obtained as

$$\begin{aligned}\dot{W}(e,\rho,\delta) \leq {}& \frac{1}{2}\sum_{i=1}^{N} e_i^T\left(PA+A^TP\right)e_i - \sum_{i=1}^{N}\sum_{j=1}^{N} a_{ij}\beta_{ij}\frac{(c_{ij}-\alpha_0)^2}{8} \\ & - \sum_{i=1}^{N}\sum_{j=1}^{N} a_{ij}\alpha_0\left(\alpha_{ij} - \frac{1-\mu_{ij}}{\gamma_{ij}}\right)\delta_{ij} \\ & - \alpha_0\left(\frac{1}{4}-\iota\right)\sum_{i=1}^{N}\sum_{j=1}^{N} a_{ij}\tilde{\eta}_{ij}^T\Gamma\tilde{\eta}_{ij} + \varsigma. \end{aligned}\tag{24}$$

Since $\tilde{\eta}_{ij} = \tilde{\theta}_i^j - \tilde{\theta}_j^i = (e_i^j + \theta_i) - (e_j^i + \theta_j) = (e_i^j - e_j^i) + (\theta_i - \theta_j)$, by using Young's inequality, one can deduce

$$\begin{aligned}&\sum_{i=1}^{N}\sum_{j=1}^{N} a_{ij}(\theta_i-\theta_j)^T\Gamma(\theta_i-\theta_j) \\ &= \sum_{i=1}^{N}\sum_{j=1}^{N} a_{ij}\tilde{\eta}_{ij}^T\Gamma\tilde{\eta}_{ij} - \sum_{i=1}^{N}\sum_{j=1}^{N} a_{ij}(e_i^j-e_j^i)^T\Gamma(e_i^j-e_j^i) \\ &\quad - 2\sum_{i=1}^{N}\sum_{j=1}^{N} a_{ij}(\theta_i-\theta_j)^T\Gamma(e_i^j-e_j^i) \\ &\leq \sum_{i=1}^{N}\sum_{j=1}^{N} a_{ij}\tilde{\eta}_{ij}^T\Gamma\tilde{\eta}_{ij} + \sum_{i=1}^{N}\sum_{j=1}^{N} a_{ij}(e_i^j-e_j^i)^T\Gamma(e_i^j-e_j^i) \\ &\quad + \frac{1}{2}\sum_{i=1}^{N}\sum_{j=1}^{N} a_{ij}(\theta_i-\theta_j)^T\Gamma(\theta_i-\theta_j). \end{aligned}\tag{25}$$

Thus, it is easy to obtain that

$$\begin{aligned} e^T(\mathscr{L}\otimes\Gamma)e =& \frac{1}{2}\sum_{i=1}^{N}\sum_{j=1}^{N} a_{ij}(e_i-e_j)^T\Gamma(e_i-e_j) \\ =& \frac{1}{2}\sum_{i=1}^{N}\sum_{j=1}^{N} a_{ij}(\theta_i-\theta_j)^T\Gamma(\theta_i-\theta_j) \\ \le& \sum_{i=1}^{N}\sum_{j=1}^{N} a_{ij}\tilde{\eta}_{ij}^T\Gamma\tilde{\eta}_{ij}+4\sum_{i=1}^{N}\sum_{j=1}^{N} a_{ij}e_i^{jT}\Gamma e_i^j. \quad (26) \end{aligned}$$

According to (10), we have $\dot{c}_{ij}\ge -\pi_{ij}\beta_{ij}c_{ij}$, $\forall t\ge 0$, and thus $c_{ij}\ge c_{ij}(0)\exp\{-\pi_{ij}\beta_{ij}t\}>0$, $\forall t\ge 0$. Therefore, from the dynamic event-triggering condition (11), we have

$$a_{ij}e_i^{jT}\Gamma e_i^j-\iota_{ij}a_{ij}\tilde{\eta}_{ij}^T\Gamma\tilde{\eta}_{ij}\le a_{ij}\frac{\delta_{ij}}{\gamma_{ij}}. \quad (27)$$

In addition, let $q_0=\max\left\{1+4\iota,\frac{4}{\gamma q_1}\right\}$ and $q_1\le \min_{(i,j)\in\mathscr{E}}\left\{\frac{1}{2}\left(\alpha_{ij}-\frac{1-\mu_{ij}}{\gamma_{ij}}\right)/(\frac{1}{4}-\iota)\right\}$ with $\gamma=\min_{(i,j)\in\mathscr{E}}\{\gamma_{ij}\}$. Substituting (27) into (26) gives

$$\begin{aligned} e^T(\mathscr{L}\otimes\Gamma)e \le& \sum_{i=1}^{N}\sum_{j=1}^{N}(1+4\iota_{ij})a_{ij}\tilde{\eta}_{ij}^T\Gamma\tilde{\eta}_{ij}+4\sum_{i=1}^{N}\sum_{j=1}^{N} a_{ij}\frac{\delta_{ij}}{\gamma_{ij}} \\ \le& q_0\sum_{i=1}^{N}\sum_{j=1}^{N} a_{ij}\tilde{\eta}_{ij}^T\Gamma\tilde{\eta}_{ij}+q_0q_1\sum_{i=1}^{N}\sum_{j=1}^{N} a_{ij}\delta_{ij}. \quad (28) \end{aligned}$$

Therefore,

$$\sum_{i=1}^{N}\sum_{j=1}^{N} a_{ij}\tilde{\eta}_{ij}^T\Gamma\tilde{\eta}_{ij}\ge \frac{1}{q_0}e^T(\mathscr{L}\otimes\Gamma)e-q_1\sum_{i=1}^{N}\sum_{j=1}^{N} a_{ij}\delta_{ij}. \quad (29)$$

Denote $\tilde{\alpha}_0=\frac{\alpha_0(1-4\iota)}{2q_0}$. Then, (24) can be rewritten as

$$\begin{aligned} \dot{W}(e,\rho,\delta)\le& \frac{1}{2}e^T\left[\mathrm{I}_N\otimes\left(PA+A^TP\right)-\tilde{\alpha}_0\mathscr{L}\otimes\Gamma\right]e \\ &-\frac{1}{2}\sum_{i=1}^{N}\sum_{j=1}^{N} a_{ij}\alpha_0\left(\alpha_{ij}-\frac{1-\mu_{ij}}{\gamma_{ij}}\right)\delta_{ij} \\ &-\sum_{i=1}^{N}\sum_{j=1}^{N} a_{ij}\beta_{ij}\frac{(c_{ij}-\alpha_0)^2}{8}+\varsigma. \quad (30) \end{aligned}$$

Moreover, $\tilde{\alpha}_0\lambda_2\ge 1$ due to $\alpha_0\ge\frac{2q_0}{(1-4\iota)\lambda_2}$. Thus, from (15), we get that

$$\begin{aligned} \dot{W}(e,\rho,\delta)\le& \frac{1}{2}\sum_{i=1}^{N} e_i^T\left(PA+A^TP-PBB^TP\right)e_i \\ &-\frac{1}{2}\sum_{i=1}^{N}\sum_{j=1}^{N} a_{ij}\alpha_0\left(\alpha_{ij}-\frac{1-\mu_{ij}}{\gamma_{ij}}\right)\delta_{ij} \\ &-\sum_{i=1}^{N}\sum_{j=1}^{N} a_{ij}\beta_{ij}\frac{(c_{ij}-\alpha_0)^2}{8}+\varsigma \\ \le& -\kappa_1 W(e,\rho,\delta)+\varsigma, \quad (31) \end{aligned}$$

where $\kappa_1=\min_{(i,j)\in\mathscr{E}}\left\{\beta_{ij}\pi_{ij},\frac{\alpha_{ij}}{2}-\frac{1-\mu_{ij}}{2\gamma_{ij}},\frac{\sigma_1}{\lambda_{\max}(P)}\right\}>0$.

Now we consider the case $t\in\overline{\mathscr{A}}(t_1,t_2)$, over which communication channels are subject to DoS attacks. Consider the same Lyapunov function $W(e,\rho,\delta)$ as (22). Under DoS attacks, we have $a_{ij}=0$, $\forall(i,j)\in\mathscr{E}$. Thus, the time derivative of $W(e,\rho,\delta)$ can be obtained as

$$\begin{aligned} \dot{W}(e,\rho,\delta)\le& \frac{1}{2}\sum_{i=1}^{N} e_i^T(t)(PA+A^TP)e_i(t) \\ \le& \frac{\sigma_2}{2}\sum_{i=1}^{N} e_i^TPe_i\le\kappa_2 W(e,\rho,\delta(t)), \quad (32) \end{aligned}$$

where $\kappa_2=\sigma_2>0$.

Assume that there is no DoS attacks at the start time instant. For easier understanding, the time interval without/with DoS attacks can be rewritten as $\cup_{k\in\mathbb{N}}[t_{2k},t_{2k+1})$ and $\cup_{k\in\mathbb{N}}[t_{2k+1},t_{2k+2})$, which represent $\overline{\mathscr{A}}(t_1,t_2)$ and $\overline{\mathscr{A}}^c(t_1,t_2)$, respectively.

For simplicity and clarity, we rewrite $W(e,\rho,\delta)$ as $W(t)$. From (31) and (32), we get that

$$\dot{W}(t)\le\begin{cases}-\kappa_1W(t)+\varsigma, & t\in[t_{2k},t_{2k+1}),\\ \kappa_2W(t), & t\in[t_{2k+1},t_{2k+2}).\end{cases} \quad (33)$$

Then, in terms of the comparison method, we get the following solution of (33)

$$W(t)\le\begin{cases}e^{-\kappa_1(t-t_{2k})}W(t_{2k})+\int_{t_{2k}}^{t}e^{-\kappa_1(t-\tau)}\varsigma d\tau, & t\in[t_{2k},t_{2k+1}),\\ e^{\kappa_2(t-t_{2k+1})}W(t_{2k+1}), & t\in[t_{2k+1},t_{2k+2}).\end{cases} \quad (34)$$

By interation over (34), we have the following result

$$\begin{aligned} W(t)\le& e^{-\kappa_1|\overline{\mathscr{A}}^c(t_0,t)|+\kappa_2|\overline{\mathscr{A}}(t_0,t)|}W(t_0) \\ &+\varsigma\int_{t_0}^{t}e^{-\kappa_1|\overline{\mathscr{A}}^c(\tau,t)|+\kappa_2|\overline{\mathscr{A}}(\tau,t)|}d\tau. \quad (35) \end{aligned}$$

In fact, UAVs need time to recover communication, which is denoted by Δ. In combination with Assumption 2 , we have $|\overline{\mathscr{A}}(t_0,t)|\le T_0+\frac{t-t_0}{\tau_a}+N_f(t_0,t)\Delta$. Thus,

$$\begin{aligned} -\kappa_1|\overline{\mathscr{A}}^c(t_0,t)|+\kappa_2|\overline{\mathscr{A}}(t_0,t)|\le& -\kappa_1(t-t_0) \\ &+(\kappa_1+\kappa_2)\left(T_0+\frac{t-t_0}{\tau_a}+N_f(t_0,t)\Delta\right). \quad (36) \end{aligned}$$

Therefore, from (35) and (36), we have

$$\begin{aligned} W(t)\le& e^{-\eta(t-t_0)}e^{(\kappa_1+\kappa_2)T_0}W(t_0)+\frac{\varsigma}{\eta}e^{(\kappa_1+\kappa_2)T_0}(1-e^{-\eta(t-t_0)}) \\ =& ce^{-\eta(t-t_0)}W(t_0)+\frac{\varsigma}{\eta}e^{(\kappa_1+\kappa_2)T_0}, \quad (37) \end{aligned}$$

where $\eta=\kappa_1-\frac{\kappa_1+\kappa_2}{\tau_a}-\kappa^*>0$ and $c=e^{(\kappa_1+\kappa_2)T_0}(1-\frac{\varsigma}{\eta W(t_0)})$. The inequality (37) implies that $W(t)$ is bounded. Thus, e_i, c_{ij}, and δ_{ij} are bounded and the desired formation configuration is achieved.

Secondly, we discuss the exclusion of Zeno behavior.

Note that the error $e_i^j(t)=\tilde{\theta}_i^j(t)-\theta_i(t)$ for agent i is not continuous and reset to zero at the triggering moments $\{t_k^{i\to j}\}$. Consider the right-hand Dini derivative of $e_i^j(t)$ for $t\in[t_k^{i\to j},t_{k+1}^{i\to j})$, $t_{k+1}^{i\to j}<\infty$, thus, from (5), (7), and (13), we get that

$$D^+e_i^j(t)=Ae_i^j(t)-BK\sum_{i=1}^{N}a_{ij}c_{ij}\tilde{\eta}_{ji}(t). \quad (38)$$

Since $e_i(t)$ is bounded, we can see that $\theta_i(t) - \theta_j(t)$ is bounded. Moreover, $\tilde{\eta}_{ij}(t) = \tilde{\theta}_i^j(t) - \tilde{\theta}_j^i(t) = e^{A(t-t_k^{i\to j})}\theta_i(t_k^{i\to j}) - e^{A(t-t_{k'}^{j\to i})}\theta_j(t_{k'}^{j\to i})$ is bounded, where $t_{k'}^{j\to i}$ represents the lastest event-triggering time instant of agent j to agent i. Then, it is easily obtained that

$$D^+\|e_i^j(t)\| \le \|A\|\|e_i^j(t)\| + \bar{\sigma}_{ij}, \tag{39}$$

where $\bar{\sigma}_{ij}$ denotes the upper bound of $\|BK\|\sum_{i=1}^N a_{ij}\bar{c}\|\tilde{\eta}_{ji}(t)\|$ and $\bar{c}$ represents the upper bound of c_{ij} since c_{ij} is also bounded. Denote by $\Phi : [0,\infty) \to \mathbb{R}_{\ge 0}$ a non-negative function satisfying

$$\dot{\Phi}(t) = \|A\|\Phi(t) + \bar{\sigma}_{ij}, \tag{40}$$

with $\Phi(0) = \|e_i^j(t_k^{i\to j})\| = 0$. Then, we have that $\|e_i^j(t)\| \le \Phi(t - t_k^{i\to j})$ with $\Phi(t) = \frac{\bar{\sigma}_{ij}}{\|A\|}(e^{\|A\|t} - 1)$. From the dynamic event-triggering condition (11), we obtain that

$$\|e_i^j(t)\|^2 \le \frac{1}{\gamma_{ij}(1+\varepsilon_{ij}c_{ij}(t))\|\Gamma\|}\delta_{ij}(t). \tag{41}$$

According to (41), we get that the interval between two triggering instants $t_k^{i\to j}$ and $t_{k+1}^{i\to j}$ for agent i can be lower bounded by the time for $\Phi^2(t - t_k^{i\to j})$ evolving from 0 to $\frac{\delta_{ij}(0)}{\gamma_{ij}(1+\varepsilon_{ij}\bar{c})\|\Gamma\|}\exp\{-(\alpha_{ij} + \frac{\mu_{ij}}{\gamma_{ij}})t\}$, which is the lower bound of the right-hand side of (41). Thus, a lower bound Δ_k^{ij} of $t_{k+1}^{i\to j} - t_k^{i\to j}$ can be gotten by solving the inequality below

$$\begin{aligned}&\frac{\bar{\sigma}_{ij}^2}{\|A\|^2}(e^{\|A\|\Delta_k^{ij}} - 1)^2 \\ \ge&\frac{\delta_{ij}(0)}{\gamma_{ij}(1+\varepsilon_{ij}\bar{c})\|\Gamma\|}\exp\{-(\alpha_{ij} + \frac{\mu_{ij}}{\gamma_{ij}})(t_k^{i\to j} + \Delta_k^{ij})\}.\end{aligned} \tag{42}$$

Then, it is obtained that

$$t_{k+1}^{i\to j} - t_k^{i\to j} \ge \Delta_k^{ij} \ge \frac{1}{\|A\|}\ln\left(1 + \frac{\|A\|}{\bar{\sigma}_{ij}}\varkappa_{ij}\right), \tag{43}$$

where $\varkappa_{ij} = \sqrt{\frac{\delta_{ij}(0)}{\gamma_{ij}(1+\varepsilon_{ij}\bar{c})\|\Gamma\|}\exp\{-(\alpha_{ij} + \frac{\mu_{ij}}{\gamma_{ij}})(t_k^{i\to j} + \Delta_k^{ij})\}}$. Here, notice that the right-hand side of the second inequality in (43) approaches zero only when $t \to \infty$. In this case, $t_k^{i\to j} \to \infty$ with $k \to \infty$ and $t \to \infty$. Besides, $t_{k+1}^{i\to j} - t_k^{i\to j} \ge \Delta_k^{ij} > 0$ exists in any finite time. Thus, it can be concluded that Zeno behavior does not exist for each agent of the MAS in any finite time.

REFERENCES

[1] D. N. Das, R. Sewani, J. Wang, and M. K. Tiwari, "Synchronized truck and drone routing in package delivery logistics," *IEEE Transactions on Intelligent Transportation Systems*, vol. 22, no. 9, pp. 5772–5782, 2020.

[2] P. K. R. Maddikunta, S. Hakak, M. Alazab, S. Bhattacharya, T. R. Gadekallu, W. Z. Khan, and Q.-V. Pham, "Unmanned aerial vehicles in smart agriculture: Applications, requirements, and challenges," *IEEE Sensors Journal*, vol. 21, no. 16, pp. 17 608–17 619, 2021.

[3] D. A. Saikin, T. Baca, M. Gurtner, and M. Saska, "Wildfire fighting by unmanned aerial system exploiting its time-varying mass," *IEEE Robotics and Automation Letters*, vol. 5, no. 2, pp. 2674–2681, 2020.

[4] P. Petráček, V. Krátkỳ, M. Petrlík, T. Báča, R. Kratochvíl, and M. Saska, "Large-scale exploration of cave environments by unmanned aerial vehicles," *IEEE Robotics and Automation Letters*, vol. 6, no. 4, pp. 7596–7603, 2021.

[5] R. Cajo, M. Guinaldo, E. Fabregas, S. Dormido, D. Plaza, R. De Keyser, and C. Ionescu, "Distributed formation control for multi-agent systems using a fractional-order proportional–integral structure," *IEEE Transactions on Control Systems Technology*, vol. 29, no. 6, pp. 2738–2745, 2021.

[6] J. Wang, L. Han, X. Li, X. Dong, Q. Li, and Z. Ren, "Time-varying formation of second-order discrete-time multi-agent systems under non-uniform communication delays and switching topology with application to uav formation flying," *IET Control Theory & Applications*, vol. 14, no. 14, pp. 1947–1956, 2020.

[7] Q. Li, J. Wei, Q. Gou, and Z. Niu, "Distributed adaptive fixed-time formation control for second-order multi-agent systems with collision avoidance," *Information Sciences*, vol. 564, pp. 27–44, 2021.

[8] R. Ringbäck, J. Wei, E. S. Erstorp, J. Kuttenkeuler, T. A. Johansen, and K. H. Johansson, "Multi-agent formation tracking for autonomous surface vehicles," *IEEE Transactions on Control Systems Technology*, vol. 29, no. 6, pp. 2287–2298, 2020.

[9] W. Zhao, W. Yu, and H. Zhang, "Observer-based formation tracking control for leader–follower multi-agent systems," *IET Control Theory & Applications*, vol. 13, no. 2, pp. 239–247, 2019.

[10] S. J. Yoo and T.-H. Kim, "Distributed formation tracking of networked mobile robots under unknown slippage effects," *Automatica*, vol. 54, pp. 100–106, 2015.

[11] S. Zuo, Y. Song, F. L. Lewis, and A. Davoudi, "Time-varying output formation containment of general linear homogeneous and heterogeneous multiagent systems," *IEEE Transactions on Control of Network Systems*, vol. 6, no. 2, pp. 537–548, 2018.

[12] X. Dong, Y. Hua, Y. Zhou, Z. Ren, and Y. Zhong, "Theory and experiment on formation-containment control of multiple multirotor unmanned aerial vehicle systems," *IEEE Transactions on Automation Science and Engineering*, vol. 16, no. 1, pp. 229–240, 2018.

[13] Y. Hua, X. Dong, L. Han, Q. Li, and Z. Ren, "Formation-containment tracking for general linear multi-agent systems with a tracking-leader of unknown control input," *Systems & Control Letters*, vol. 122, pp. 67–76, 2018.

[14] C. Gudla, M. S. Rana, and A. H. Sung, "Defense techniques against cyber attacks on unmanned aerial vehicles," in *Proceedings of the international conference on embedded systems, cyber-physical systems, and applications (ESCS)*. The Steering Committee of The World Congress in Computer Science, Computer Engineering and Applied Computing (WorldComp), 2018, pp. 110–116.

[15] F. Alrefaei, A. Alzahrani, H. Song, and S. Alrefaei, "A survey on the jamming and spoofing attacks on the unmanned aerial vehicle networks," in *2022 IEEE International IOT, Electronics and Mechatronics Conference (IEMTRONICS)*. IEEE, 2022, pp. 1–7.

[16] B. Ly and R. Ly, "Cybersecurity in unmanned aerial vehicles (UAVs)," *Journal of Cyber Security Technology*, vol. 5, no. 2, pp. 120–137, 2021.

[17] D. Zhang, L. Liu, and G. Feng, "Consensus of heterogeneous linear multiagent systems subject to aperiodic sampled-data and DoS attack," *IEEE Transactions on Cybernetics*, vol. 49, no. 4, pp. 1501–1511, 2018.

[18] D. Zhang, Y.-P. Shen, S.-Q. Zhou, X.-W. Dong, and L. Yu, "Distributed secure platoon control of connected vehicles subject to DoS attack: Theory and application," *IEEE Transactions on Systems, Man, and Cybernetics: Systems*, vol. 51, no. 11, pp. 7269–7278, 2020.

[19] X. Wang, J. H. Park, and H. Yang, "An improved protocol to consensus of delayed mass with unms and aperiodic DoS cyber-attacks," *IEEE Transactions on Network Science and Engineering*, vol. 8, no. 3, pp. 2506–2516, 2021.

[20] L. Ding, Q.-L. Han, X. Ge, and X.-M. Zhang, "An overview of recent advances in event-triggered consensus of multiagent systems," *IEEE Transactions on Cybernetics*, vol. 48, no. 4, pp. 1110–1123, 2017.

[21] D. Zhang, Y. Tang, Z. Ding, and F. Qian, "Event-based resilient formation control of multiagent systems," *IEEE Transactions on Cybernetics*, vol. 51, no. 5, pp. 2490–2503, 2019.

[22] W. Zhang, Y. Tang, Y. Liu, and J. Kurths, "Event-triggering containment control for a class of multi-agent networks with fixed and switching topologies," *IEEE Transactions on Circuits and Systems I: Regular Papers*, vol. 64, no. 3, pp. 619–629, 2017.

[23] B. Cheng and Z. Li, "Coordinated tracking control with asynchronous edge-based event-triggered communications," *IEEE Transactions on Automatic Control*, vol. 64, no. 10, pp. 4321–4328, 2019.

[24] R. A. Horn and C. R. Johnson, *Matrix analysis*. Cambridge University Press, 2012.